Jacek LISTWAN, Krzysztof PIENKOWSKI

Department of Electrical Machines, Drives and Measurements, Wroclaw University of Science and Technology

doi:10.15199/48.2020.10.02

Comparison of DFOC of Seven-Phase Induction Motor with PI and Fuzzy-Logic speed Controller under speed sensor fault

Abstract*. The paper presents the analysis of the Direct Field-Oriented Control of seven-phase squirrel-cage induction motor with the application of the PI and Fuzzy-Logic controller in the speed control loop and with MRAS^{CC} estimator. The encoder failure in the DFOC control system has been analyzed. The mathematical model of the seven-phase induction motor has been presented and the MRAS^{CC} estimator has been described. The descriptions of the Space Vector Modulation and Fuzzy-Logic controller have been shown. Results of simulation studies of the Direct Field-Oriented Control methods in the speed sensor fault condition are presented.*

Streszczenie. *W artykule przedstawiono analizę metody bezpośredniego sterowania polowo-zorientowanego siedmiofazowym silnikiem indukcyjnym klatkowym z zastosowaniem regulatora PI i regulatora rozmytego w pętli regulacji prędkości i z zastosowaniem estymatora MRAS^{CC}. Analizowano awarię enkodera w układzie sterowania DFOC. Opisano model matematyczny 7-fazowego silnika indukcyjnego i opisano estymator MRAS^{CC}. Przedstawiono opis zastosowanej metody modulacji wektorowej i regulatora rozmytego. Przedstawiono wyniki badań symulacyjnych analizowanej metody sterowania w stanie awarii czujnika prędkości.* ***(Porównanie sterowania DFOC siedmio-fazowym silnikiem indukcyjnym z zastosowaniem regulatorów PI i regulatora rozmytego w stanie awarii czujnika prędkości)***

Keywords: seven-phase squirrel-cage induction motor, MRAS^{CC} estimator, Direct Field-Oriented Control method, Fault Tolerant Control
Słowa kluczowe: 7-fazowy silnik indukcyjny klatkowy, estymator MRAS^{CC}, bezpośrednie sterowanie polowo-zorientowane, sterowanie odporne na uszkodzenia

Introduction

Nowadays, the development of modern power electronics, makes possible to consider the motor with the number of stator phases greater than three. The interest in induction motors with more than three phases has increased, especially for high-power applications. The multiphase motors have a lot of advantages in comparison with conventional three-phase motors [1, 3-6, 10], for example: reducing the amplitude and increasing the frequency of torque pulsations, reducing the rotor harmonic currents losses, lowering the dc link current harmonics and improved reliability. The other important cause is that for given motor power, an increase of the number of phases enables the reduction of power per phase, that is the reduction of power per inverter leg.

In the literature the different control methods of the multiphase motors have been discussed [1, 3-6, 10]. In this paper the system of Direct Field-Oriented Control of seven-phase induction motor has been considered and described. In the presented control system the Stator-Current-Based Model Reference Adaptive System (MRAS^{CC}) estimator has been applied [8]. The application of this estimation system allows for the elimination of the mechanical sensors and increasing of the reliability of the drive system with seven-phase induction motor. The Fuzzy-Logic controller in the speed control loop has been also applied in one of the analyzed DFOC systems. This type of controller can give much better control results in comparison with conventional linear controllers [2, 9].

This article presents the analysis of seven-phase induction motor with Direct Field-Oriented Control (DFOC) during the state of the occurrence of the encoder failure. The comparison of impact of this fault-state has been analyzed for the DFOC with linear PI controller and for DFOC with Fuzzy-Logic controller in the speed control loop.

Mathematical model of seven-phase induction motor

The mathematical model of the seven-phase induction motor has been formulated on the basis of commonly used simplifying assumptions [1, 3-6, 10]. The analysis and control of this type of motor in the stator and rotor phase coordinate system is difficult, because the obtained motor model is described by the equations with the time dependent coefficients. For this reason, the appropriate transformation matrices [4, 5] are applied and a model of the seven-phase induction motor with constant coefficients is obtained.

After transformations the original seven-phase system of stator and rotor is decomposed into three orthogonal subspaces: the α-β, $z1$-$z2$, $z3$-$z4$ and the system of zero components. The stator and rotor α-β components are next transformed to the common x-y orthogonal system, which is rotating with arbitrary angular speed ω_k relative to the stator [4, 5].

The general equations of seven-phase induction motor after transformation take the following form [4, 5]:

- the voltage equations of the stator and rotor in the common rotating x-y coordinate system:

$$u_{sx} = R_s\, i_{sx} - \omega_k\, \psi_{sy} + \frac{d}{dt}\psi_{sx} \tag{1}$$

$$u_{sy} = R_s\, i_{sy} + \omega_k\, \psi_{sx} + \frac{d}{dt}\psi_{sy} \tag{2}$$

$$0 = R_r\, i_{rx} - (\omega_k - \omega_e)\psi_{ry} + \frac{d}{dt}\psi_{rx} \tag{3}$$

$$0 = R_r\, i_{ry} + (\omega_k - \omega_e)\psi_{rx} + \frac{d}{dt}\psi_{ry} \tag{4}$$

- the stator voltage equations in the additional coordinate systems $z1$-$z2$ and $z3$-$z4$:

$$u_{sz1} = R_s\, i_{sz1} + \frac{d}{d}\psi_{sz1} \tag{5}$$

$$u_{sz2} = R_s\, i_{sz2} + \frac{d}{dt}\psi_{sz2} \tag{6}$$

$$u_{sz3} = R_s\, i_{sz3} + \frac{d}{dt}\psi_{sz3} \tag{7}$$

$$u_{sz4} = R_s\, i_{sz4} + \frac{d}{dt}\psi_{sz4} \tag{8}$$

- the equation of the motor electromagnetic torque:

(9) $$T_e = \frac{7}{2} \cdot p_b \cdot \frac{L_m}{L_r}\left(\psi_{rx} i_{sy} - \psi_{ry} i_{sx}\right)$$

where: u_{sx}, u_{sy}, u_{sz1}, u_{sz2}, u_{sz3}, u_{sz4} - components of the stator voltage vectors in the x-y, $z1$-$z2$ and $z3$-$z4$ coordinate systems; i_{sx}, i_{sy}, i_{sz1}, i_{sz2}, i_{sz3}, i_{sz4}, i_{rx}, i_{ry} - components of the stator and rotor current vectors in the x-y, $z1$-$z2$ and $z3$-$z4$ coordinate systems; ψ_{sx}, ψ_{sy}, ψ_{sz1}, ψ_{sz2}, ψ_{sz3}, ψ_{sz4}, ψ_{rx}, ψ_{ry} - components of the stator and rotor flux linkage vectors in the x-y, $z1$-$z2$ and $z3$-$z4$ coordinate systems; ω_e - the electrical angular speed of the motor; T_e - the motor electromagnetic torque; R_s, R_r - stator and rotor phase resistance; L_m - motor magnetizing inductance; L_r - rotor inductance; p_b - the number of motor pole pairs.

The variables considered in the coordinate systems $z1$-$z2$ and $z3$-$z4$ do not contribute in energy conversion and in generation of motor torque. However the stator components in these systems must be minimized with the use of the appropriate space vector modulation, because they can cause enlargement of the amplitude of the stator phase currents and extra power losses in the stator windings [1, 3-6, 10]. The rotor components in the $z1$-$z2$ and $z3$-$z4$ systems. and the stator and rotor zero components are always equal to zero because the rotor is short-circuited and the stator is assumed to be star-connected with isolated neutral point. Because of this, the equations for these components are neglected in the further analysis.

Space Vector Modulation method

In the research presented in this article it was assumed, that the considered seven-phase induction motor is supplied by the two-level seven-phase Voltage Source Inverter (VSI). The seven-phase VSI generates 2^7=128 output stator voltage space vectors. In the set of all generated voltage vectors, 126 active vectors and 2 zero vectors can be identified. The active space vectors have different magnitudes and there are 14 sectors that can be identified [1, 5].

Stator voltage space vectors generated by the seven-phase Voltage Source Inverter in the coordinate system α-β are presented in Figure 1a, in the coordinate system $z1$-$z2$ are presented in Figure 1b and in the coordinate system $z3$-$z4$ are presented in the Figure 1c. All voltage space vectors presented in Fig. 1 have been identified with decimal numbers and these numbers can be converted into seven-position binary numbers. These binary numbers determine the states of the individual switches of the seven-phase VSI.

a)

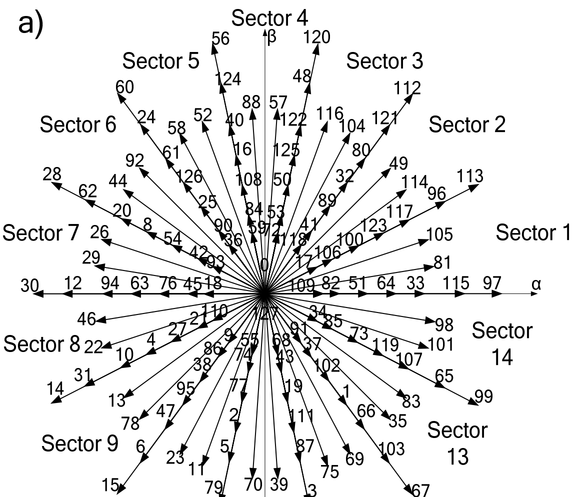

b)

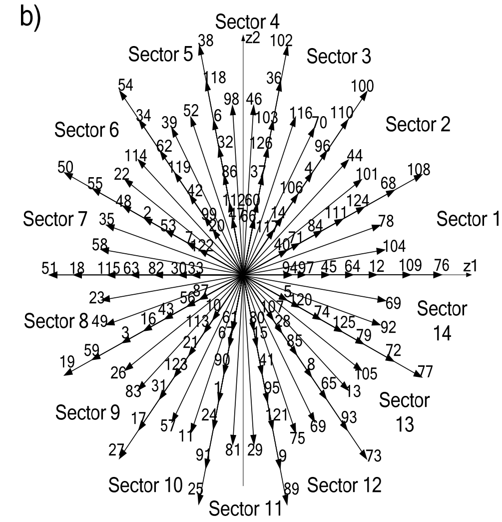

c)

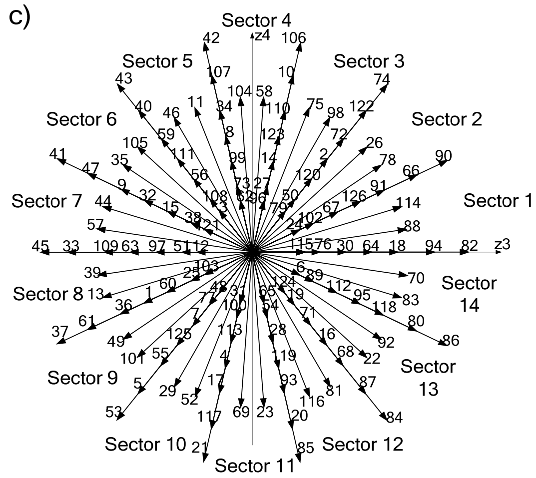

Fig.1. Voltage space vectors generated by the seven-phase Voltage Source Inverter in coordinate systems:
a) α-β, b) $z1$-$z2$, c) $z3$-$z4$

In the selected concept of Space Vector Modulation method the six active space vectors and two zero vectors are selected per switching period to achieve the given voltage vector. Graphical interpretation of the concept of Space Vector Modulation method has been presented in the Figure 2. The voltage space vectors in the α-β plane and the case when the reference voltage vector $\underline{u}_{sref}$ is situated in Sector 1 are considered [1, 5].

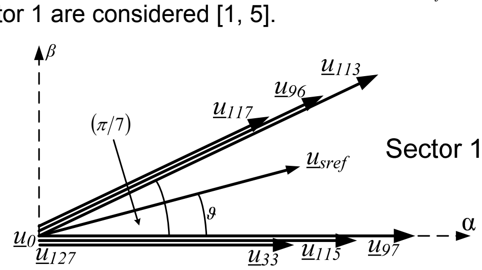

Fig.2. The principle of determining the reference voltage vector with the choice of six active voltage vectors

In this case the reference voltage vector is synthesized by using six active voltage vectors: two short vectors: $\underline{u}_{33}$, $\underline{u}_{117}$, two medium vectors: $\underline{u}_{96}$, $\underline{u}_{115}$, two long vectors: $\underline{u}_{97}$, $\underline{u}_{113}$ and two zero voltage vectors: u_0, u_{127}. This concept of Space Vector Modulation allows to achieve the reference voltage vector in the α-β plane and at the same time to achieve the zero values of voltage vectors in the additional *z1-z2* and z3-z4 planes [1, 5].

Switching times of voltage vectors are calculated according to the equations [1, 5]:

(10) $$t_{a1} = \sin(3\pi/7)\cdot\sin(s\cdot\pi/7-\vartheta)\cdot\frac{u_{sref}}{u_d}\cdot T_s$$

(11) $$t_{a2} = \sin(2\pi/7)\cdot\sin(s\cdot\pi/7-\vartheta)\cdot\frac{u_{sref}}{u_d}\cdot T_s$$

(12) $$t_{a3} = \sin(\pi/7)\cdot\sin(s\cdot\pi/7-\vartheta)\cdot\frac{u_{sref}}{u_d}\cdot T_s$$

(13) $$t_{b1} = \sin(3\pi/7)\cdot\sin[\vartheta-(s-1)\cdot\pi/7]\cdot\frac{u_{sref}}{u_d}\cdot T_s$$

(14) $$t_{b2} = \sin(2\pi/7)\cdot\sin[\vartheta-(s-1)\cdot\pi/7]\cdot\frac{u_{sref}}{u_d}\cdot T_s$$

(15) $$t_{b3} = \sin(\pi/7)\cdot\sin[\vartheta-(s-1)\cdot\pi/7]\cdot\frac{u_{sref}}{u_d}\cdot T_s$$

(16) $$t_0 = T_s - (t_{a1}+t_{b1}+t_{a2}+t_{b2}+t_{a3}+t_{b3})$$

where: t_{a1}, t_{b1} - switching time of long active voltage vectors; t_{a2}, t_{b2} - switching time of medium voltage vectors; t_{a3}, t_{b3} - switching time of short voltage vectors; t_0 - switching time of zero voltage vectors; u_{sref} - magnitude of the reference voltage vector; T_s - switching period; ϑ - the angle of position of reference voltage vector; s – number of sector.

Fuzzy - Logic controller

The Fuzzy-Logic controller in the speed control loop has been applied in one of the analyzed DFOC systems with seven-phase induction motor. The general diagram of the applied Fuzzy-Logic Controller (FLC) has been presented in the Figure 3 [2, 9].

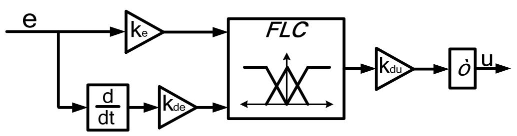

Fig.3. The general diagram of the Fuzzy-Logic Controller

The block diagram of the Fuzzy-Logic Controller has been presented in the Figure 4 [2, 9].

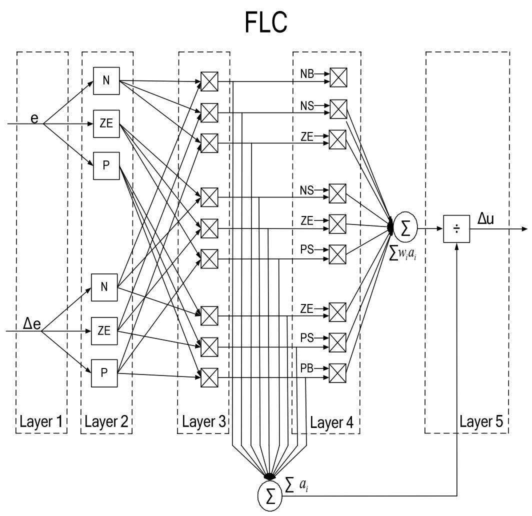

Fig.4. The block diagram of the Fuzzy-Logic Controller

The structure of Fuzzy-Logic Controller has been divided into five control Layers [2, 9]:

- Layer 1 is responsible for calculation of two control signals. The first input control signal e is the difference between the reference and estimated motor speed. The second input control signal Δe is the time derivative of the first input signal. In this layer of the FLC, the k_e and k_{de} scalling factors are used.
- In the Layer 2 the output signals from Part 1 are fuzzified with the use of the appropriate membership functions.
- The multiplication of the appropriate output signals from Part 2 is carried out in Layer 3. In this part the "prod" function is used.
- Layer 4 is responsible for multiplication of the activation levels of the rules and member functions. The member functions were chosen as: N (negative), ZE (zero), P (positive), NB (negative big), NS (negative small), PS (positive small), PB (positive big). Multiplication in this part of the Fuzzy-Logic Controller take place in accordance with the multiplication rules. Linguistic Rule Table applied in Fuzzy-Logic Controller is presented in Table 1.

Table 1. Linguistic Rule Table

		Δe		
		N	ZE	P
e	N	NB	NS	ZE
	ZE	NS	ZE	PS
	P	ZE	PS	PB

- Layer 5 is responsible for calculation of the output signal u from FLC. The output signal is calculated according to the method of Center of Gravity. In this layer of the FLC, the k_{du} scalling factor is used.

MRAS^{CC} estimator

The MRAS^{CC} estimator has been used to the reproduction of the speed signal of the seven-phase induction motor and the rotor flux vector in the DFOC control systems with the seven-phase induction motor, resistant to the damage of the motor speed sensor. It is an adaptive estimator in which the model of the induction motor is implemented as the reference model. The block scheme of the MRAS^{CC} estimator is presented in Fig. 5 [8].

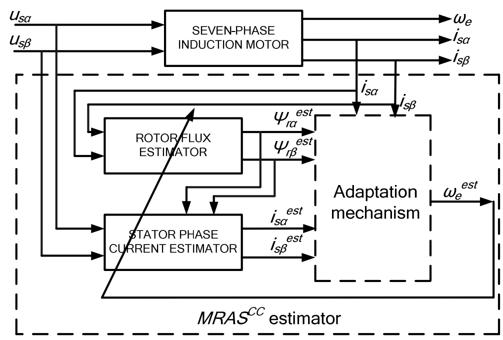

Fig.5. The block scheme of the MRAS^{CC} estimator

The stator phase currents of the seven-phase induction motor are measured and the components of the stator current vector in the α-β coordinate system are afterwards determined. These components are compared to the components reproduced by using the stator current-voltage model of the induction motor [8]. The rotor flux vector estimator [7] is tuned by the angular speed signal of the rotor of the induction motor, determined by the adaptation algorithm. The estimator of the stator current vector can be obtained with using the voltage model and the current model of the rotor flux estimator [8]. The operation of the estimator of the stator current vector depends on the values: components of a stator voltage vector, components of a rotor flux vector and the rotor angular speed.

The errors between the estimated stator current values and the measured values are used in the motor speed reproduction algorithm, which can be defined as follows [8]:

$$\omega_e^{est} = K_p \cdot \left(e_{i_{s\alpha}} \cdot \psi_{r\beta} - e_{i_{s\beta}} \cdot \psi_{r\alpha}\right) + \frac{1}{T_i}\int \left(e_{i_{s\alpha}} \cdot \psi_{r\beta} - e_{i_{s\beta}} \cdot \psi_{r\alpha}\right)dt \quad (17)$$

where: $e_{i_{s\alpha}} = i_{s\alpha} - i_{s\alpha}^{est}$, $e_{i_{s\beta}} = i_{s\beta} - i_{s\beta}^{est}$ represent the errors between the measured and estimated values of the components of the stator current vector in the α-β coordinate system; K_p, T_i are the coefficients of the proportional and integral parts of the PI controller.

DFOC control method

The scheme of the Direct Field-Oriented Control (DFOC) of seven-phase squirrel-cage induction motor with MRAS[CC] speed estimator, linear PI controllers and Fuzzy-Logic Controller in the speed control loop is shown in Figure 6.

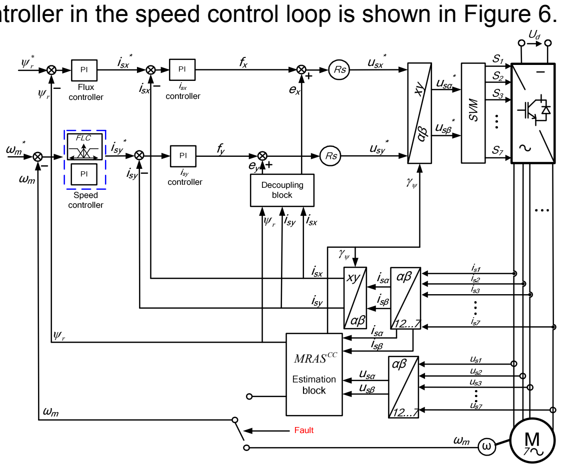

Fig.6. The DFOC control system of seven-phase induction motor

The MRAS[CC] estimator determines the estimated value of motor angular speed (ω_m^{est}) and the instantaneous magnitude of the rotor flux vector (ψ_r^{est}). In the considered DFOC control structure four control loops are applied: the control loop for motor angular speed with PI or Fuzzy-Logic controller, the control loop for magnitude of the rotor flux vector with PI controller and two control loops for x and y component of stator current vector. The reference values of the stator voltage vector components determined in the x-y coordinate system are transformed to the α-β coordinate system and are given to the Space Vector Modulation (SVM) block. The Space Vector Modulator sets the switching states of the seven-phase Voltage Source Inverter. In order to improve the dynamical properties of the drive systems, the decoupling blocks have been also applied in the control systems [7].

Simulation results

Simulation studies were carried out for the seven-phase squirrel-cage induction motor with the following data and parameters: f_N=50Hz, p_b=2, R_s=10Ω, R_r=6.3Ω, L_{ls}=L_{lr}=0.04H, L_m=0.42H.

In the simulation tests, it was assumed, that damage of the speed sensor occurs at any time during start-up of the seven-phase induction motor. The failure of the speed sensor is detected by the appropriate diagnostic system. After this failure the signal obtained from the motor speed sensor was replaced by the estimated speed signal. The estimated speed signal was delivered through the designed MRAS[CC] estimator. The simulation studies have been performed for the DFOC method with PI controllers and for the DFOC method with Fuzzy-Logic Controller in the speed control loop.

The waveforms of the reference speed ω_m^* (black color), simulated speed ω_{mm} (blue color) and estimated speed ω_{mest} (green color) of the seven-phase induction motor for the analyzed DFOC methods are presented in the Figure 7.

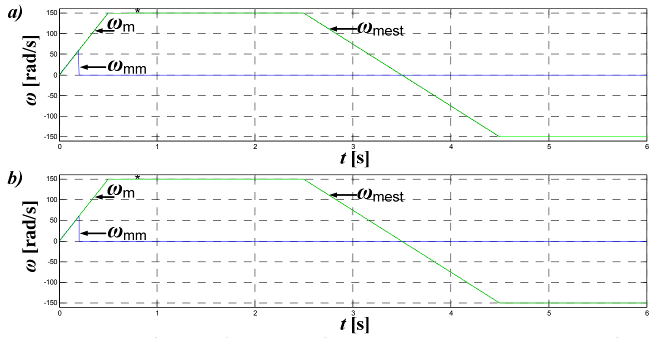

Fig.7. The waveforms of speeds of seven-phase induction motor for DFOC method with: a) PI controllers; b) FLC speed controller

Based on the analysis of the results of simulation studies, it can be stated that the both DFOC methods provides accurate control of the induction motor speed before the occurrence of the speed sensor failure and after the failure and switching the control system to the sensorless speed control. The decrease of the measured motor speed to a value equal to zero after the failure of the speed sensor has been visible. The time of switching to sensorless speed control is not noticeable in the waveform of the estimated speed for both analyzed DFOC methods.

The waveforms of the load torque T_m and the electromagnetic torque T_e of seven-phase induction motor for DFOC methods are presented in the Figure 8 and the waveforms of the y component of the stator current vector of the seven-phase induction motor for the DFOC methods have been shown in Figure 9.

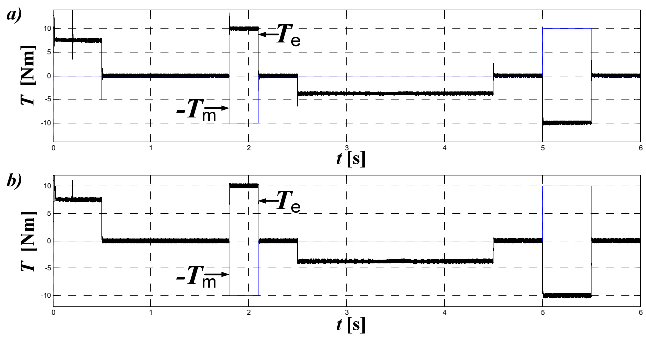

Fig.8. The waveforms of load torque and electromagnetic torque of seven-phase induction motor for DFOC method with: a) PI controllers; b) FLC speed controller

The analysis of the obtained simulation results allows to state that oscillations and overshoots in the waveform of the motor electromagnetic torque and in the waveform of the y current component are smaller for the DFOC method with FLC applied in the speed control loop.

The waveforms of the all stator phase currents of seven-phase induction motor for the considered control systems are presented in the Figure 10. The amplitudes of the stator phase currents depend on the state of the drive system and the value of the load torque.

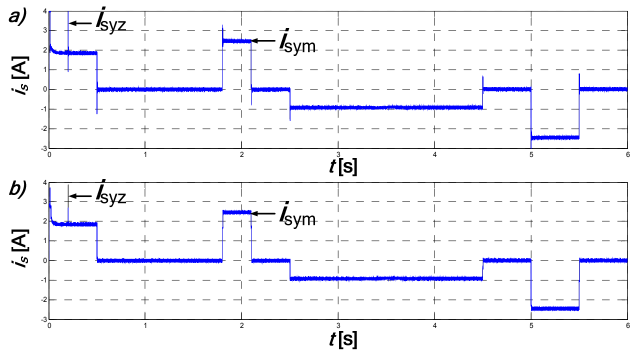

Fig.9. The waveforms of the y current component of seven-phase induction motor for DFOC method with: a) PI controllers; b) FLC speed controller

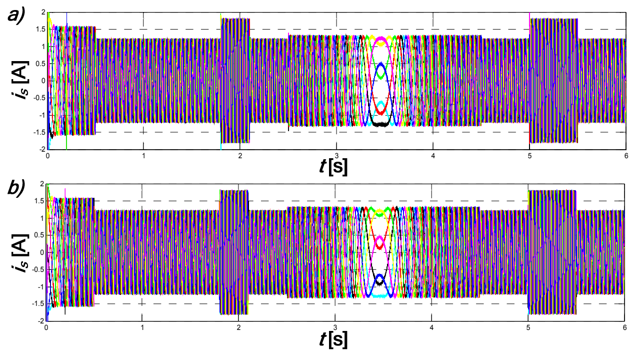

Fig.10. The stator phase currents of the seven-phase motor for DFOC method with: a) PI controllers; b) FLC speed controller

In the Figure 11 the trajectories of the current components in the α-β, $z1$-$z2$ and $z3$-$z4$ coordinate systems are presented. The components of the stator current vector in the $z1$-$z2$ and $z3$-$z4$ coordinate systems reach small values in comparison with the values of the stator current components in the α-β coordinate system.

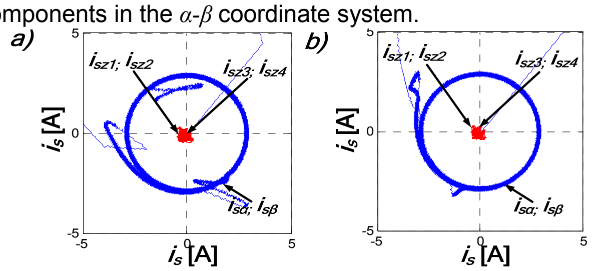

Fig.11. The trajectories of the components of the stator phase currents of the seven-phase motor for DFOC method with: a) PI controllers; b) FLC speed controller

The trajectories of the estimated magnitude of the rotor flux vector is presented in Figure 12. It can be stated, that the rotor flux vector is controlled properly at the nominal value for both analyzed DFOC methods.

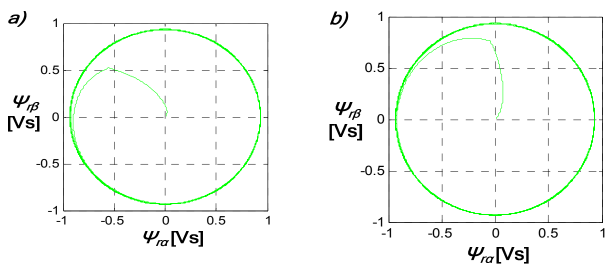

Fig.12. The trajectories of the estimated magnitude of the rotor flux vector of the seven-phase motor for DFOC method with: a) PI controllers; b) FLC speed controller

Conclusions

The mathematical model of the seven-phase squirrel-cage induction motor has been presented. The description of the Space Vector Modulation method, Fuzzy-Logic Controller and MRAS^{CC} estimator have been shown. In the Space Vector Modulation method for seven-phase VSI the long, the medium, the short and the zero voltage vectors have been used. DFOC system with a seven-phase induction motor with linear PI controllers and nonlinear Fuzzy-Logic Controller in the speed control loop has been analyzed.

The fault state in the drive system consisting in the damage of the speed sensor has been chosen to the analysis and the simulation studies for DFOC system with different controllers have been carried out. Selected results of the simulation studies are presented and discussed.

From the comparative analysis of simulation studies of DFOC with linear PI controllers and simulation studies of DFOC with Fuzzy-Logic Controller in the speed control loop follows that the DFOC with FLC provides the better accuracy of the control of variables of seven-phase induction motor.

Authors: *Jacek Listwan, Ph.D., e-mail: jacek.listwan@pwr.edu.pl, Krzysztof Pieńkowski, Ph.D., D.Sc., e-mail: krzysztof.pienkowski@pwr.edu.pl, Wroclaw University of Science and Technology, Faculty of Electrical Engineering, Department of Electrical Machines, Drives and Measurements, 19 Smoluchowskiego St., 50-372 Wroclaw.*

REFERENCES

[1] Dujic D., Jones M., Levi E.: Generalised space vector PWM for sinusoidal output voltage generation with multiphase voltage source inverters, *Int. J. Industrial Electronics and Drives* (2009), Vol. 1, No. 1, 1-13
[2] El-Barbary Z. M. S.: Fuzzy logic based controller for five-phase induction motor drive system, *Alexandria Engineering Journal* (2012), No. 51, 263-268
[3] Iqbal A., Levi E., Space Vector PWM Techniques for Sinusoidal Output Voltage Generation with a Five-Phase Voltage Source Inverter, *Electric Power Components and System*, (2006), Vol. 34, No. 2, 119-140
[4] Levi E., Bojoi R., Profumo F., Toliyat H. A., Wiliamson S., Multiphase induction motor drives - a technology status review, *IET Electr. Power Appl*, (2007), 489-516
[5] Listwan J., Direct Torque Control of Multi-Phase Induction Motor with Fuzzy-Logic Speed Controller, *Informatyka, Automatyka, Pomiary w Gospodarce i Ochronie Środowiska,(2017),* vol. 4, 38-43
[6] Listwan J., Pienkowski K., DTC-ST and DTC-SVM Control of Five-Phase Induction Motor with MRAS^{CC} estimator, *Przegląd Elektrotechniczny,(2016),* R.92, nr 11, 252-256
[7] Orlowska-Kowalska T., Sensorless Induction Motor Drive, *Wroclaw University of Technology Press,* (2003), Wroclaw (in Polish)
[8] Orlowska-Kowalska T., Dybkowski M., Stator-Current-Based MRAS Estimator for a Wide Range Speed-Sensorless Induction Motor Drive, *IEEE Transaction on Industrial Electronics*, (2010), Vol. 57, No. 4, 1296-1308,
[9] Orlowska-Kowalska T., Szabat K., Optimization of Fuzzy-Logic Speed Controller for DC Drive System With Elastic Joints, *IEEE Transaction on Industry Applications*, (2004), Vol. 40, No. 4, 1138-1144,
[10] Zhao Y., Lipo T.A.: Space vector PWM Control of Dual Three-Phase Induction Machine Using Vector Space Decomposition. *IEEE Transaction on Industry Applications*, (1995), Vol. 31, No. 5, 1100-1109.